Iranian Journal of Remote Sensing & GIS. *2026, 18 (2): 97-114* P-ISSN: 2008-5966, E-ISSN: 2588-6185

Original Article

Refinement of Road Extraction Based on Deep Learning Methods in UAV Images

Fatemeh Bozorgian and Hadiseh Hasani*

Affiliation
Dep of Geodesy and Surveying Engineering, Tafresh University, Tafresh, Iran

ABSTRACT

Road extraction from remotely sensed images plays an important role in urban planning, navigation systems, traffic management, mapping, and monitoring. In the last decade, several advanced machine learning methods have been developed alongside data acquisition technologies. In this study, a new post-processing method is developed to enhance the results of convolutional neural networks (CNNs) by injecting spatial information. For this purpose, Xception, a powerful deep learning network, is implemented to extract roads in UAV images. Although it detects the road accurately, there are still false positive and negative pixels in the classification map. In this study, a post-processing step based on spatial information is proposed to decrease the FP and FN. Several morphological operators are considered in this step, and the road boundaries with their direction are also computed. The fusion of the obtained results based on Xception and the spatial information of the post-processing stage significantly improves the road extraction results. The proposed method was evaluated using the NITR and UDD datasets. The obtained results on NITR show that Xception achieved 93.81%, while UNet and SegNet achieved 85.97% and 77.11%, respectively. On the UDD dataset, XCeption achieved 91.94%, whereas UNet and SegNet achieved 83.19% and 75.67%, respectively. The proposed method can improve the Xception results by up to 96.08% and 94.47%, respectively.

Keywords: Road extraction, Deeplab v3+, road boundaries, refinement, and UAV images.

* Corresponding Author: h.hasani@tafreshu.ac.ir
DOI: https://doi.org/10.48308/gisj.2026.240326.1271
Received: 2025.06.11
Accepted: 2026.05.31

Copyright: © 2026 by the authors. Submitted for possible open access publication under the terms and conditions of the Creative Commons Attribution (CC BY) license https://creativecommons.org/licenses/by/4.0/).

1. Introduction

Nowadays, road extraction is one of the most important analyses of remote sensing data (Z. Chen et al., 2022). This process involves the identification and separation of roads from other natural and artificial features in aerial or satellite images. Owing to the growing demand for accurate and up-to-date information for urban management, transportation planning, and infrastructure monitoring, automatic and semi-automatic road extraction has become increasingly important (Li et al., 2019; Lian et al., 2020; Ural et al., 2015). These studies not only increase the speed and accuracy of spatial data analysis but also prevent the waste of human and financial resources (Herumurti et al., 2013). Although several studies have been performed, there are still several challenges, such as the proximity of trees, building shadows, similarity of roads and sidewalks, and the presence of cars on roads. Therefore, there is a wide range of research on road extraction from remotely sensed data.

The data resources applied for road sensing can be categorized into three groups: 2D (optical and radar image), 3D (terrestrial and aerial laser scanner), and hybrid (Z. Chen et al., 2022). Although LiDAR and laser scanners provide a rich source of structural data of objects, they are costly and present huge amounts of data that require high computation. On the other hand, 2D data, especially optical images, are available and less expensive. Since roads usually have specific patterns and a distinct appearance, optical images can be efficiently used for road extraction applications (Sghaier & Lepage, 2015). In recent decades, UAV platforms have been successfully applied in remote sensing applications. According to the high spatial resolution of UAV images, they can be used in road extraction with high accuracy (Kestur et al., 2018).

Road extraction methods from 2D remote sensing images are divided into three categories: morphological operations (Singh & Garg, 2013), traditional machine learning (ML) algorithms (Song & Civco, 2004), and deep learning-based methods (Liu et al., 2024). In road extraction methods, image pixels are classified into two categories: “road” and “background.” Roads are usually covered by other objects such as cars, trucks, buses, and motorcycles. In some studies, these objects are also included as part of the road. Although these objects can make the identification of road areas complicated, they also provide important contextual information that is useful for road recognition in complex situations (Alshehhi et al., 2017). To extract these features, several techniques, such as binarization, dilation, erosion, and opening and closing operations, are used. In the 1980s, researchers began to apply mathematical morphology to extract road features (Destival, 1986). However, the use of morphological features may be associated with problems such as shape bias. To solve this problem, Valero et al. (2010) introduced

an advanced directional morphological operator that exploits the opening and closing of paths to extract structural pixel information (Valero et al., 2010). These morphological operators are flexible to adapt for linear and slightly curved structures, as they do not depend on the choice of structural element shape. The method involves constructing a granulometric chain using "path opening" and "path closing" to construct morphological profiles. For each pixel, the morphological profile is considered as the feature vector used to extract roads (Courtrai & Lefèvre, 2016).

Morphological methods can extract road shape features; however, they usually have little resistance to gaps, light changes, and contrast. Consequently, ML methods have been proposed to solve these challenges. For this purpose, several textural, spectral, and structural features are manually extracted, and classifiers are used for the final classification. Linear features, such as ridges or stripes, highlight potential road areas in remote sensing images, and classic classifiers include decision trees (DT), support vector machines (SVMs), and random forest (RF).

There are a wide variety of traditional machine learning methods for road extraction from optical images. Maboudi et al. (2016) proposed multi-stage methods to extract road networks from very high-resolution satellite images. For this purpose, the images were segmented, and structural, spectral, textural, and contextual features were extracted. Subsequently, tensor voting was applied to extract the road network (Maboudi et al., 2016). Coulibaly et al. (2017) improved the road extraction quality by using Lowe's scale-invariant features transform descriptors jointly with spectral angle algorithms. They proposed a semi-automatic method to extract road networks in Quickbird images during a major disaster (Coulibaly et al., 2017). Yang et al. (2024) presented a framework for the intelligent extraction of road networks. For this purpose, spectral features were extracted using a 3D wavelet transform in the frequency domain, jointly with texture in the time domain. Subsequently, an optimized support vector machine was implemented to extract the road images more accurately (Yang et al., 2024).

Traditional machine learning methods generally perform better than methods based on morphological features. However, these methods still face challenges, such as incomplete feature coverage, weak extendibility to different data, and complexity in determining optimal parameters. To solve these problems, deep learning-based approaches have been used for road extraction. In recent years, with the development of deep learning, significant progress has been made in the field of computer vision. Most deep learning methods can be divided into convolutional neural networks (CNN), fully convolutional neural networks (FCN), autoencoders (AE), and generative adversarial networks (GAN).

Inspired by image segmentation, edge detection, and object skeleton extraction, a multi-task CNN called RoadNet is used to simultaneously predict road surfaces, edges, and central lines (Liu et al., 2018). To maintain the integrity and continuity of the extracted roads, U-Net is used, which is an extended version of a convolutional neural network (Akhtarmanesh et al., 2023). To solve the problem of imbalance data between roads and background areas, another model of a fully connected network is proposed. Because in this network, the weight of the loss function changes owing to the imbalance between roads and backgrounds, it gives more importance to less dense road areas by weighting the loss function (Zhang & Wang, 2019). In another study, a GAN-based network was designed that was capable of identifying challenging road areas, including occlusions and shadows (W. Chen et al., 2022). According to the importance of DL methods in road extraction applications, Abdollahi et al. reviewed the state of the art of this topic. They compared GAN, FCN, deconvolution networks, and patch-based CNN in UAV and Google Earth images. They showed that all methods achieved high accuracy, but the GAN achieved the highest accuracy (Abdollahi et al., 2020).

Dabra et al. evaluated the potential of three deep learning methods, including VGG19-Net, DeepLabV3+, and SegFormer-B5, in road extraction from UAV images in Bhoopal, India. The results showed that all three methods performed well (with an IOU up to 93%) when NIR and especially nDSM data are included along with RGB images (Dabra et al. 2025). Road extraction is an essential process in disaster management for identifying the fastest routes. Ceylan and Turker applied the YOLO network to extract roads from UAV images, and then four different algorithms, such as Dijkstra, were implemented to find the shortest path. They showed that YOLOv9e-seg provided the fastest and most accurate results (Ceylan and Turker, 2026). In another study, Yigit and Uysal applied a semi-automatic object-based classification on orthophoto derived from UAV images to extract road lines. They used the NIR band along with RGB images (Yigit and Uysal, 2026).

The variety of road areas in terms of their location, size, form, and color makes developing effective segmentation algorithms more difficult. Additionally, when trees or buildings are shadowed in images, the accuracy of road segmentation is compromised. Most studies focus on road identification, and accurate boundary extraction is neglected. However, road boundary identification plays an important role in many applications, such as urban mapping. We propose a framework to segment UAV images semantically, and the extracted roads are also refined by accurate spatial analysis around road boundaries. For this purpose, a novel post-processing step, including morphological operators and road direction identification, is applied to the semantic segmentation results.

2. Proposed Methodology

The main flow of the proposed semantic segmentation method for road extraction from UAV images is illustrated in Figure 1.

The proposed method contains three main steps: first, depplabv3+ is trained on the dataset, and all data are segmented semantically by the trained network. Second, the post-processing step is applied to the classification map to improve its accuracy, where two main algorithms are implemented. Finally, the classification accuracy is evaluated based on pixel-based and object-based metrics for test data.

2.1. Semantic Segmentation based on Xception

For UAV image segmentation and road extraction, we use Deeplabv3+ and mount the Xception network on it. The dataset with associated ground truth is split into training, validation, and test data. The proposed network is trained on training data, and validation data is used to prevent overfitting. This network has 170 layers and consists of the following parts, as shown in Figure 2.

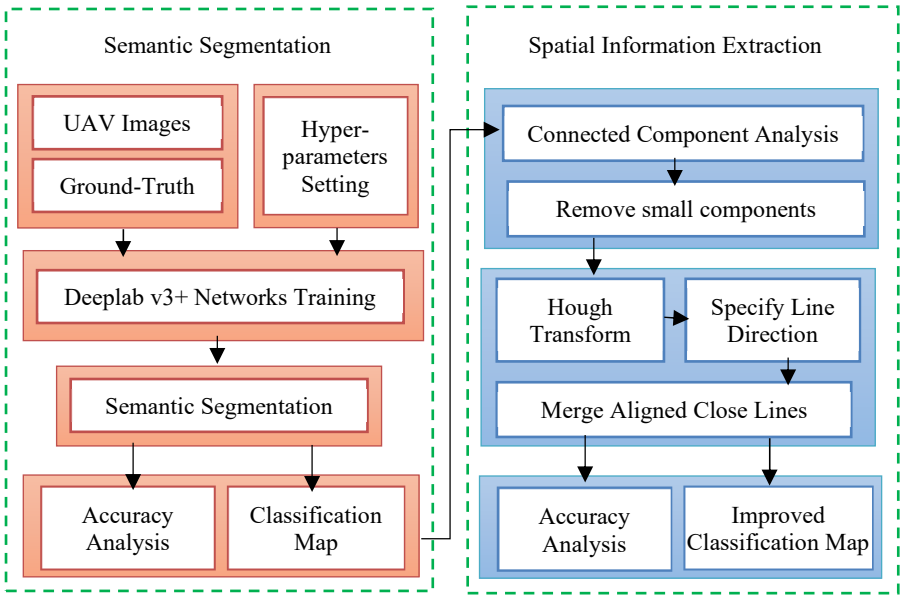


Figure 1: Flowchart of the proposed method

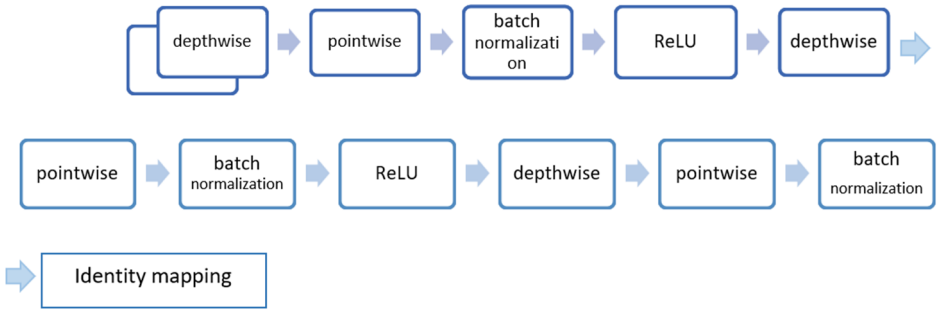


Figure 2: Architecture of the proposed network

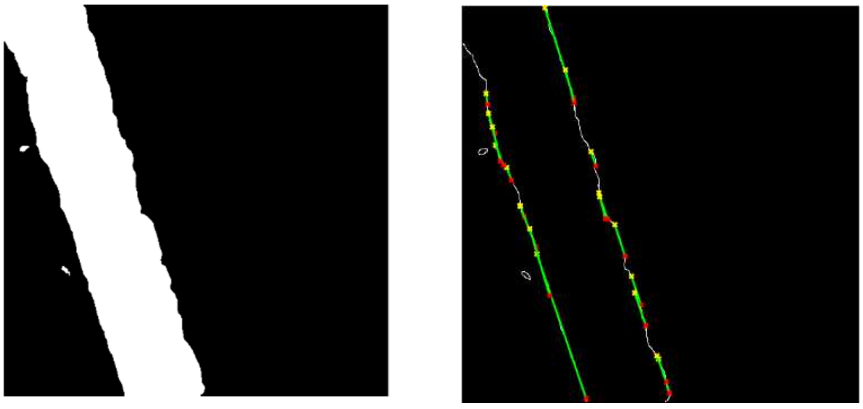
2.2. The proposed post-processing based on spatial information

In the second part of the proposed method, spatial information is extracted. For this purpose, three main preprocessing steps are considered: road boundary extraction and refinement, reclassified points near the road boundary, and morphological operations.

First, the Canny edge detector was implemented on the binary outputs of the proposed network, and the edges were identified. Then, Hough lines were created on the edges based on the two-dimensional Hough Transform (Figure 3). The slope and distance of the line from the origin were determined, and similar lines were merged. In other words, the lines that are close to each other and also have similar slopes were considered as one merged line. This step was implemented by fitting a new line to all merged pixels of selected lines based on least squares. This step creates reasonable and sufficiently large lines as road boundaries.

Secondly, in order to classify the inside, outside, and on-border pixels, the line equation ($ax + by + c = 0$) is computed for each line. Then, pixels that are close to the road boundaries are defined and their coordinates are placed in the line equation. They are classified based on their values in line equation (positive, zero and negative). Pixels that are placed inside and on the border of the road are assigned to 1 and the other ones are assigned to 0. This preserves the road-related pixels with acceptable accuracy and removes the non-road pixels near road boundaries.

In the final stage, the morphological operators are applied to remove non-road pixels and fill the road region. After applying the DL network and previous post-processing step, some pixels that do not belong to the road class but are wrongly assigned to the road class still exist. Erosion operation is considered to eliminate these pixels. Subsequently, the dilation operator is implemented to restore the road to its original shape.



(a) (b)

Figure 3: (a) Predicted classification map and (b) edge detection on the classification map.

2.3. Performance Metrics

In order to analyze the proposed method, quantitative and qualitative evaluations are implemented. The most common performance metrics in classification and object detection problems are precision, recall, accuracy, F1-score, and Dice. These metrics are formulated as Eq (1) to (5).

$$Accuracy = \frac{TP+TN}{(TP+FP+FN+TN)} \quad (1)$$

$$Precision = \frac{TP}{(TP+FP)} \quad (2)$$

$$Recall = \frac{TP}{(TP+FN)} \quad (3)$$

$$F1-score = 2 * (\frac{(Precision*Recall)}{(Precision+Recall)}) \quad (4)$$

$$Dice = \frac{2*TP}{2*TP+FP+FN} \quad (5)$$

Moreover, visual interpretation is performed for qualitative analysis. The classification and difference maps (the difference between the ground truth and predicted classification map) are depicted.

3. Experimental Results

3.1. Datasets

In this study, we used two datasets, NITRDrone and the Urban Drone Dataset (UDD). The NITRDrone dataset was collected based on the demand for scene understanding of UAV images using a semantic segmentation algorithm. This dataset contains 101 UAV images acquired using DJI-Phantom 4 and Mavic Mini. The image sizes were 1280×720, 4000×3000, and 4096×2160 pixels, and the ground sampling distance (GSD) was approximately 2.5 cm. The study area covered four classes: *road*, *vegetation*, *obstructed road,* and *background* (Behera et al., 2023). Figure 4 shows some samples of the NITRDrone dataset. The dataset was divided into training, validation, and test data. 70% of images with ground-truth are considered for training and the remaining one for the validation and evaluation step. To use all images with different sizes, we split them into 500×500 patches.

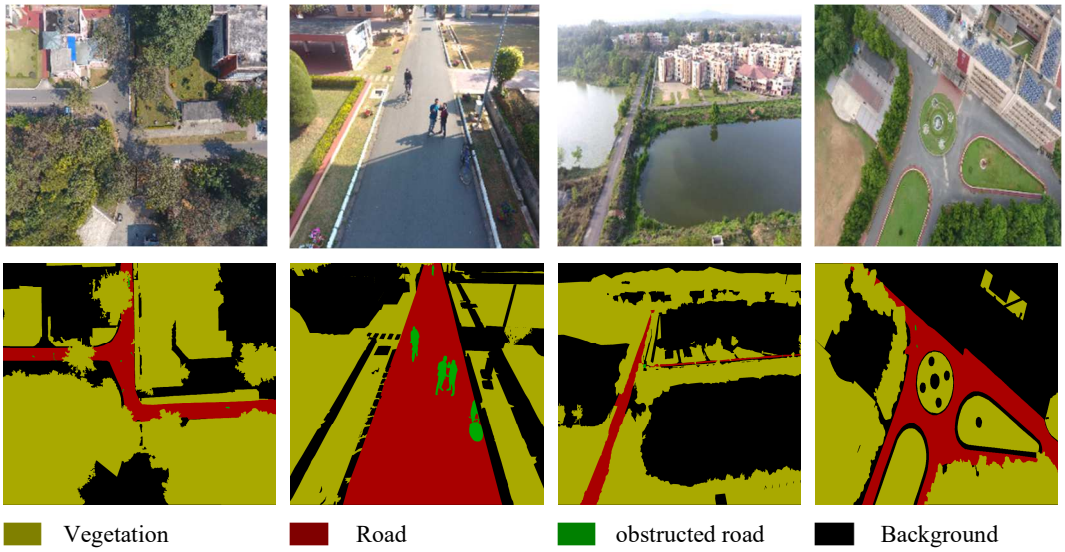


Figure 4: NITR dataset containing UAV images and ground truth.

The UDD dataset was collected by DJI-Phantom 4 in four cities in China in three subsets, UDD-3, 5, and 6, which have 3, 5, and 6 classes, respectively. In this study, UDD5, which contains *vegetation*, *road*, *building, vehicle,* and *other objects*, was used. It has 160 frames, with image sizes of 4000×3000 and 4096×2160 (Chen et al., 2018). Some samples of UDD5 are shown in Figure 5. Among 160 frames, 80 were used as training data, and the remaining ones were split into validation and test data. Similar to the NITRDrone dataset, all frames were split into 500×500 patches.

3.2. Parameters Tuning

All experiments were performed on a desktop computer equipped with an NVIDIA GeForce RTX 3090 GPU, Gen Intel® corei9 processor, and 32GB RAM. Based on this hardware configuration, the computational time of the training step was determined. Table 1 lists the hyperparameters of the proposed networks for the NITR and UDD datasets, which were defined by trial and error.

Table 1: Parameter tuning

Dataset	Parameter	Value
NTIR/UDD	Optimizer	Adam
	Batch Size	30
NITR	Max Epochs	50
UDD		200
NITR	Learning Rate	0.0001
UDD		0.001

3.3. Semantic Segmentation Results

The proposed network was trained on NITR and UDD datasets to extract roads in the UAV images. To prove the ability of the proposed method, UNet and SegNet were implemented for comparison. Table 2 lists the evaluation of the obtained results based on classification metrics.

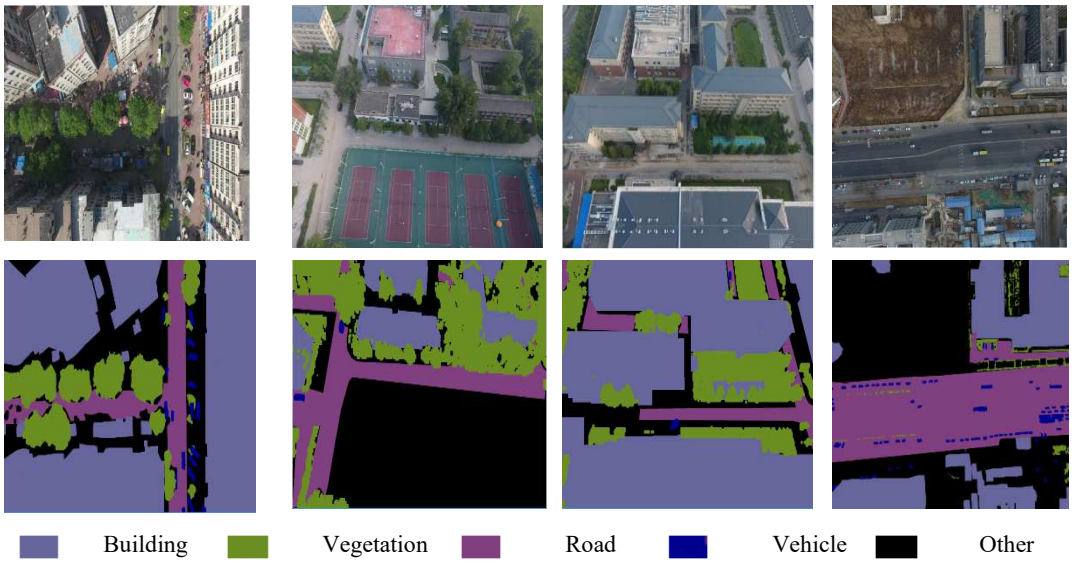


Figure 5: UDD5 dataset containing UAV images and ground truth.

Analyzing the above table shows that the proposed network outperformed all classification metrics for the NITR dataset and most metrics for the UDD dataset. However, the training time of SegNet is a bit faster than Xception. Table 3 evaluates the segmentation quality of the obtained results based on segmentation metrics.

The results in Table 3 clearly show the superiority of Xception with respect to the segmentation metric compared with UNet and SegNet. This shows that the proposed network can segment roads in UAV images with higher accuracy. In order to interpret the obtained results visually, Figure 6 and Figure 7 are depicted. As shown in these two figures, the NITR dataset is classified based on a multi-class network, and for the UDD dataset, a binary classifier is applied.

Comparing the results of the proposed method with ground truth and other methods in the NITR dataset proves the ability of Xception in extracting roads in UAV images. Xception reaches a classification map with better visual interpretation and higher spatial accuracy.

Analyzing four samples of the UDD dataset in Figure 7 shows that in complex urban area Xception still gains high accuracy and a better classification map, but UNet and SegNet have relatively poor performance. Although Xception has reasonable performance in both datasets, there are also some challenges in extracting road boundaries. Consequently, a post-processing step was implemented to improve the results.

Table 2: Classification metrics of road extraction based on the proposed network

Dataset	Method	F1-Score	Recall	Precision	Dice	Accuracy (%)	Training Time (m)
NITR	Xception	0.937	1	0.88	0.86	93.18	2454
	UNet	0.862	0.99	0.76	0.75	85.97	3007
	SegNet	0.791	0.93	0.69	0.58	77.11	2260
UDD	Xception	0.631	0.67	0.6	0.63	91.94	149
	UNet	0.094	0.23	0.06	0.1	83.19	152
	SegNet	0.514	0.36	0.91	0.48	75.67	59

Table 3: Segmentation metrics of road extraction based on the proposed network

DataSet	Method	Mean BFScore	Weighted IOU	Mean IOU	Mean Accuracy	Global Accuracy
NITR	Xception	0.69	0.83	0.74	0.82	0.89
	UNet	0.4	0.65	0.46	0.58	0.77
	SegNet	0.25	0.54	0.39	0.52	0.67
UDD	Xception	0.63	0.86	0.72	0.82	0.92
	UNet	0.47	0.79	0.56	0.62	0.88
	SegNet	0.48	0.67	0.52	0.81	0.75

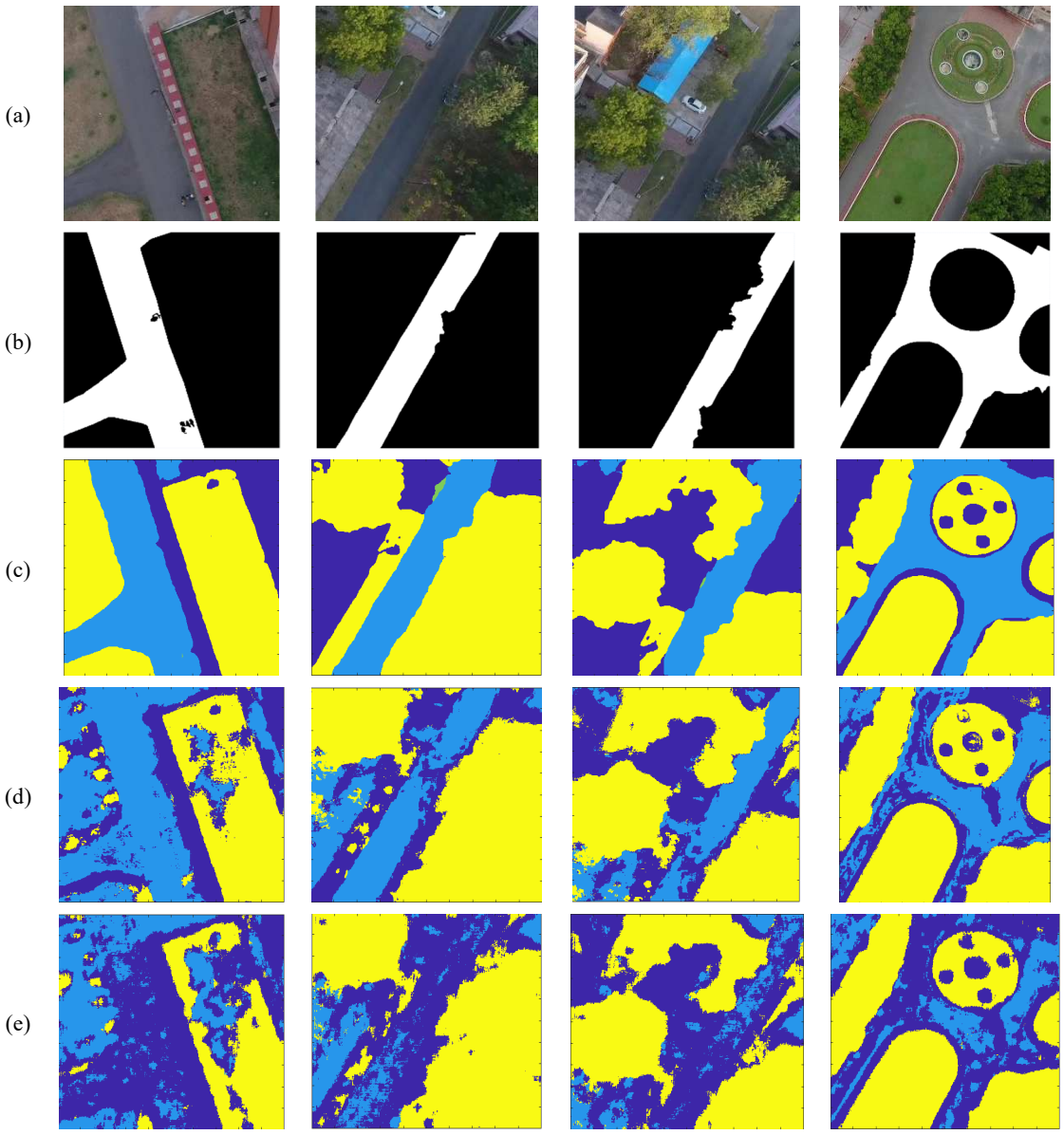


Figure 6: (a) UAV images (b) Ground-truth (c) Xception results (d) UNet results (e) SegNet results for NITR dataset.

3.4. Post-Processing Results

To improve the results of the Xception network, post-processing is implemented based on the proposed method. In Figure 8, a comparison between the Xception and the proposed methods is presented.

The above figure shows that Xception has high recall, and the proposed method reaches the same results. This means that all pixels that are predicted as road actually belong to the road class. On the other hand, the precision for Xception is 0.88, which means that there are some non-road pixels that are considered as roads. Post-processing improves this metric by up to 3%. Moreover,

the Dice metric proves that the proposed method improves the similarity of the predicted road map and the ground truth by up to 2%. Figure 9 depicts the difference classification map and ground truth in the NITR dataset.

As shown in Figure 9, the proposed method can significantly improve the classification map and make the result close to the ground truth. To prove the ability of the proposed method, it was implemented in the second dataset (UDD). Figure 10 illustrates the improvement in the post-processing step.

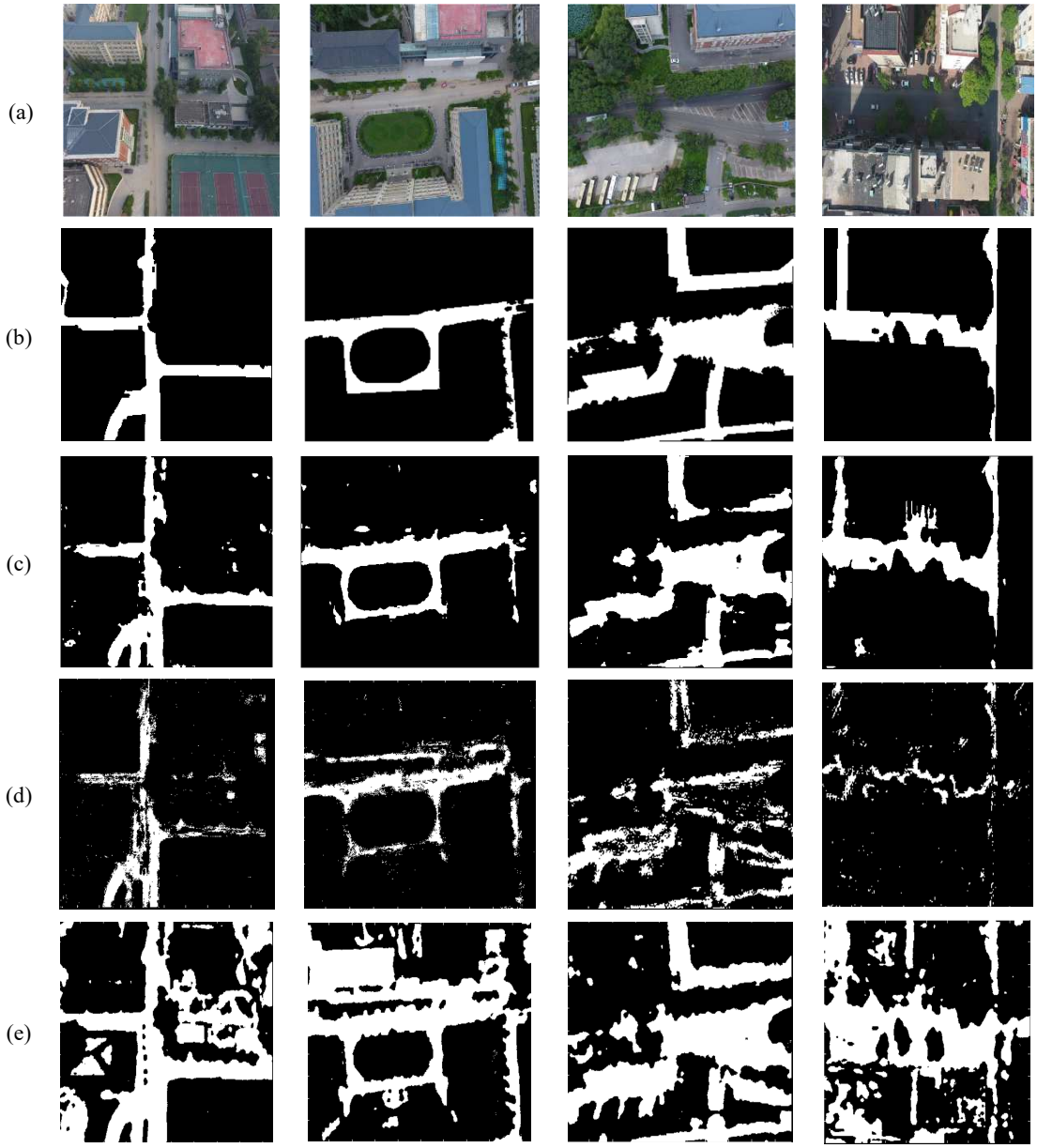


Figure 7: (a) UAV images (b) Ground-truth (c) Xception results (d) UNet results (e) SegNet results for UDD dataset.

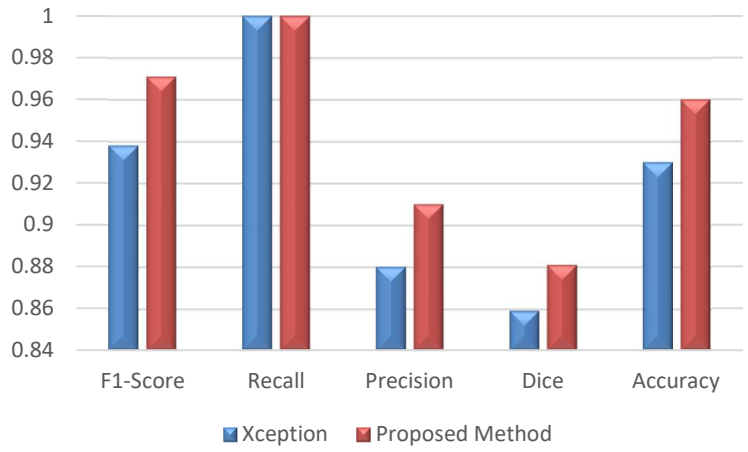


Figure 8: Accuracy of the proposed method compared with Xception in the NITR dataset.

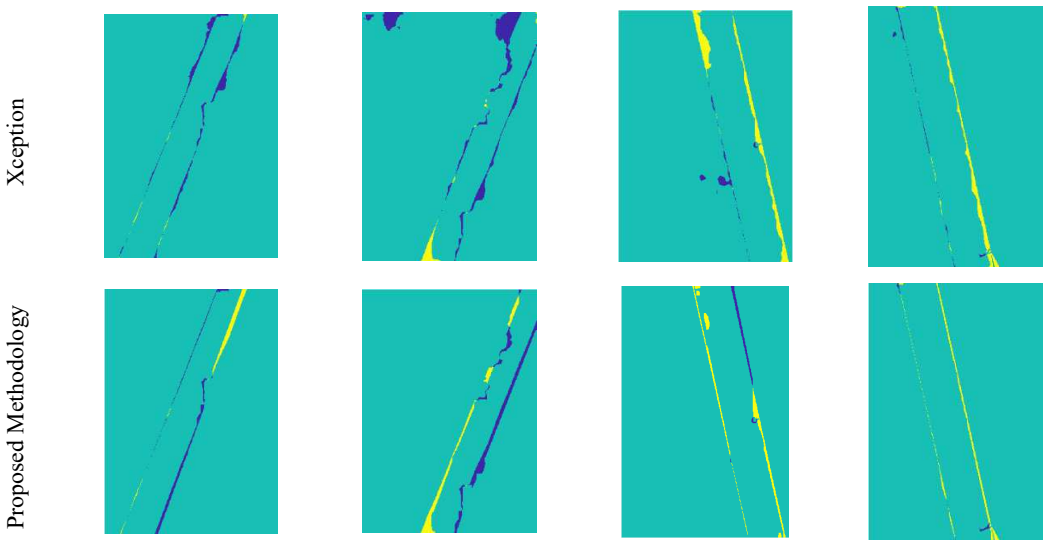


Figure 9: Difference between the predicted classification map and ground truth for the NITR dataset.

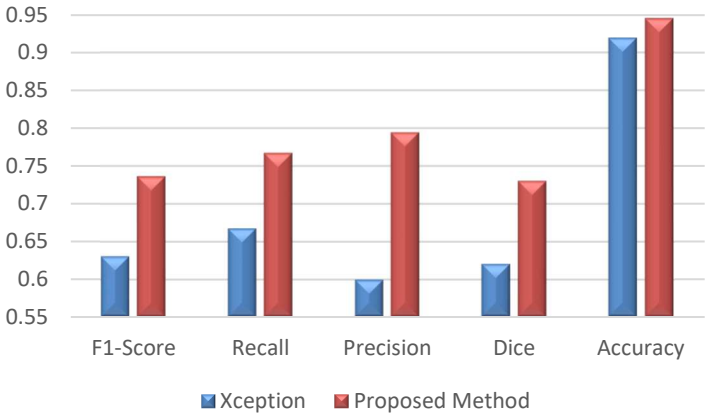


Figure 10: Accuracy of the proposed method compared with Xception in the UDD dataset.

According to the complexity of UDD, accuracy metrics reach lower values in this dataset. In this case, post-processing significantly improved the obtained results, where it improved the recall and precision of Xception, by up to 10% and 20%, respectively. This proves the high potential of the proposed method for road extraction from UAV images and improvement of deep learning methods. Comparing the recall and precision shows that more FP (samples that belong to non-road but were wrongly assigned to the road class) occurred in the results of the Xception network. The proposed post-processing step significantly eliminated these FP samples. Figure 11 illustrates the difference maps for the three samples in the UDD datasets.

A closer look at Figure 1**:** shows that although the deep learning method based on Xception can reach a reasonable accuracy, there are still several errors in their classification maps, especially in complex areas. According to the spatial characteristics of the road, the proposed post-processing step strongly improves the classification map.

4. Discussion and Conclusion

In this study, the potential of deeplabv3+ with the Xception module was evaluated for road extraction from UAV images. Its performance was compared with two standard and efficient DL networks, including UNet and SegNet. The obtained results on the NITR and UDD datasets prove the high ability of Xception in simple and complex urban areas. Its accuracy was approximately 8% and 16% more than UNet and SegNet, in both datasets. It achieved over 90% overall accuracy, but the mean IOU was 72% and 74% on NITR and UDD, respectively, and thus requires improvement.

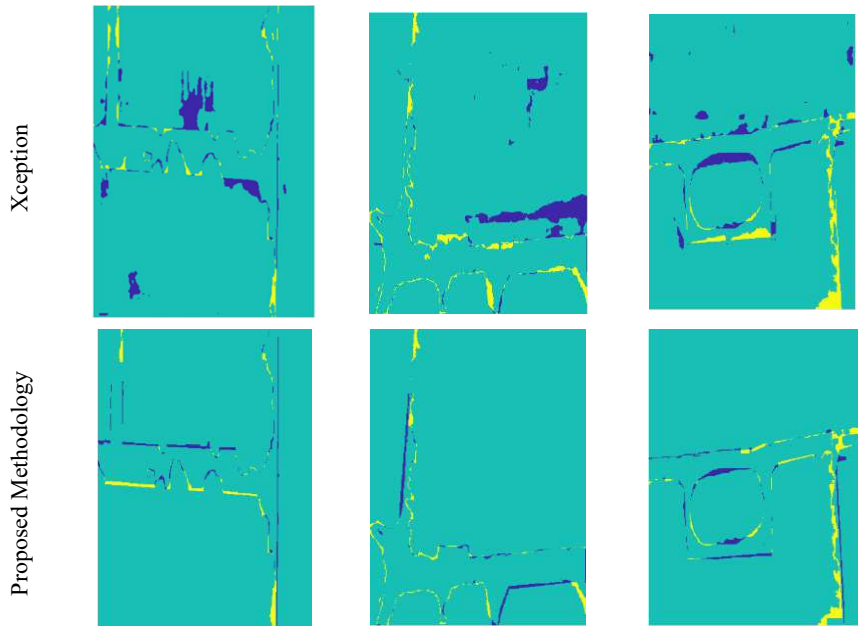


Figure 1: Difference between the predicted classification map and ground truth for the UDD dataset.

The visual evaluation of the obtained classification map showed that misclassified pixels still existed, and more spatial analysis was required. Consequently, we proposed a post-processing step containing morphological operations and road boundary analysis. First, the road boundary equation was estimated, and pixels were classified into roads and off-road areas. Then just road pixels are preserved. Subsequently, several morphological operators were applied to improve the obtained results.

The results on the UDD dataset with complex scenes show that the proposed post-processing step improves recall and precision metrics by up to 10% and 20%, respectively. According to the complexity of this dataset, Xception cannot gain high accuracy, and the obtained results based on Xception reach an F1-score of 0.63 and an accuracy of 91%. In this case, the proposed method significantly improves the obtained results. It achieves an F1-score and accuracy of 0.736 and 94.5%, respectively. Moreover, analyzing the classification map proves the ability of the proposed method to decrease FP and FN remarkably.

In the NITR dataset, which contains less complex areas, semantic segmentation networks reach high accuracies; however, there are still FP and FN, especially near road boundaries. The proposed post-processing step improves the F1-score from 0.938 to 0.971 and accuracy from 93% to 96%. The visual interpretation proves the potential of the proposed method, where FP pixels far from roads are eliminated and FP and FN pixels near roads are decreased.

However, some limitations were also observed in the proposed method, where curved or irregular boundaries were not addressed. This indicates challenges in identifying more complex and irregular patterns, which may be due to structural limitations of the model or the inherent complexities of the data. Therefore, it is necessary to investigate and develop methods and optimize algorithms in future research. Moreover, a deep learning network may be developed to extract road boundaries, and the extracted information will be fused with the deeplabv3+ results.

Data Availability

Yes

Reference

Abdollahi, A.,s Pradhan, B., Shukla, N., Chakraborty, S., & Alamri, A. (202). Deep Learning Approaches Applied to Remote Sensing Datasets for Road Extraction: A State-Of-The-Art Review. *Remote Sens*ing. 2020, 12(9), 1444. https://doi.org/10.3390/rs12091444.

Akhtarmanesh, A., Abbasi-Moghadam, D., Sharifi, A., Yadkouri, M. H., Tariq, A., & Lu, L. (2023). Road extraction from satellite images using attention-assisted UNet. *IEEE Journal of Selected Topics in Applied Earth Observations and Remote Sensing*, *17*, 1126-1136. https://doi.org/10.1109/jstars.2023.3336924

Alshehhi, R., Marpu, P. R., Woon, W. L., & Dalla Mura, M. (2017). Simultaneous extraction of roads and buildings in remote sensing imagery with convolutional neural networks. *ISPRS Journal of Photogrammetry and Remote Sensing*, *130*, 139-149. https://doi.org/10.1016/j.isprsjprs.2017.05.002

Behera, T. K., Bakshi, S., Sa, P. K., Nappi, M., Castiglione, A., Vijayakumar, P., & Gupta, B. B. (2023). The NITRDrone dataset to address the challenges for road extraction from aerial images. *Journal of Signal Processing Systems*, *95*(2), 197-209. https://doi.org/10.1007/s11265-022-01777-0.

Ceylan, M. S., & Türker, G. F. (2026). Deep Learning-Based Road Optimization Using UAVs for Disaster Areas. *Concurrency and Computation: Practice and Experience,* 38(1), e70539, https://doi.org/10.1002/cpe.70539.

Chen, W., Zhou, G., Liu, Z., Li, X., Zheng, X., & Wang, L. (2022). NIGAN: A framework for mountain road extraction integrating remote sensing road-scene neighborhood probability enhancements and improved conditional generative adversarial network. *IEEE Transactions on Geoscience and Remote Sensing*, *60*, 1-15. https://doi.org/10.1109/tgrs.2022.3188908

Chen, Y., Wang, Y., Lu, P., Chen, Y., & Wang, G. (2018). Large-scale structure from motion with semantic constraints of aerial images. Pattern Recognition and Computer Vision: First Chinese Conference, PRCV 2018, Guangzhou, China, November 23-26, 2018, Proceedings, Part I 1, https://doi.org/10.1007/978-3-030-03398-9_30

Chen, Z., Deng, L., Luo, Y., Li, D., Junior, J. M., Gonçalves, W. N., Nurunnabi, A. A. M., Li, J., Wang, C., & Li, D. (2022). Road extraction in remote sensing data: A survey. *International journal of applied earth observation and geoinformation*, *112*, 102833. https://doi.org/10.1016/j.jag.2022.102833

Coulibaly, I., Spiric, N., Lepage, R., & St-Jacques, M. (2017). Semiautomatic road extraction from VHR images based on multiscale and spectral angle in case of earthquake. *IEEE Journal of Selected Topics in Applied Earth Observations and Remote Sensing*, *11*(1), 238-248. https://doi.org/10.1109/jstars.2017.2760282.

Courtrai, L., & Lefèvre, S. (2016). Morphological path filtering at the region scale for efficient and robust road network extraction from satellite imagery. *Pattern Recognition Letters*, *83*, 195-204. https://doi.org/10.1016/j.patrec.2016.05.014.

Dabra, A., Kumar, V., & Aryal, J. (2025). Road extraction in diverse urban environments using UAV data and nDSM perturbations: A case of Bhopal, India. *Remote Sensing Applications: Society and Environment*, 37, 101465. https://doi.org/10.1016/j.rsase.2025.101465.

Destival, I. (1986). Mathematical morphology applied to remote sensing. *Acta Astronautica*, *13*(6-7), 371-385. https://doi.org/10.1016/0094-5765(86)90092-5

Herumurti, D., Uchimura, K., Koutaki, G., & Uemura, T. (2013). Urban road extraction based on hough transform and region growing. The 19th Korea-Japan Joint Workshop on Frontiers of Computer Vision, https://doi.org/10.1109/fcv.2013.6485491

Kestur, R., Farooq, S., Abdal, R., Mehraj, E., Narasipura, O., & Mudigere, M. (2018). UFCN: A fully convolutional neural network for road extraction in RGB imagery acquired by remote sensing from an unmanned aerial

vehicle. *Journal of Applied Remote Sensing*, *12*(1), 016020-016020. https://doi.org/10.1117/1.jrs.12.016020

Li, Y., Peng, B., He, L., Fan, K., Li, Z., & Tong, L. (2019). Road extraction from unmanned aerial vehicle remote sensing images based on improved neural networks. *Sensors*, *19*(19), 4115. https://doi.org/10.3390/s19194115

Lian, R., Wang, W., Mustafa, N., & Huang, L. (2020). Road extraction methods in high-resolution remote sensing images: A comprehensive review. *IEEE Journal of Selected Topics in Applied Earth Observations and Remote Sensing*, *13*, 5489-5507. https://doi.org/10.1109/jstars.2020.3023549

Liu, R., Wu, J., Lu, W., Miao, Q., Zhang, H., Liu, X., Lu, Z., & Li, L. (2024). A Review of Deep Learning-Based Methods for Road Extraction from High-Resolution Remote Sensing Images. *Remote Sensing*, *16*(12), 2056. https://doi.org/10.3390/rs16122056

Liu, Y., Yao, J., Lu, X., Xia, M., Wang, X., & Liu, Y. (2018). RoadNet: Learning to comprehensively analyze road networks in complex urban scenes from high-resolution remotely sensed images. *IEEE Transactions on Geoscience and Remote Sensing*, *57*(4), 2043-2056. https://doi.org/10.1109/tgrs.2018.2870871

Maboudi, M., Amini, J., Hahn, M., & Saati, M. (2016). Road network extraction from VHR satellite images using context aware object feature integration and tensor voting. *Remote Sensing*, *8*(8), 637. https://doi.org/10.3390/rs8080637

Sghaier, M. O., & Lepage, R. (2015). Road extraction from very high resolution remote sensing optical images based on texture analysis and beamlet transform. *IEEE Journal of Selected Topics in Applied Earth Observations and Remote Sensing*, *9*(5), 1946-1958. https://doi.org/10.1109/jstars.2015.2449296

Singh, P. P., & Garg, R. D. (2013). Automatic road extraction from high resolution satellite image using adaptive global thresholding and morphological operations. *Journal of the Indian Society of Remote Sensing*, *41*, 631-640. https://doi.org/10.1007/s12524-012-0241-4

Song, M., & Civco, D. (2004). Road extraction using SVM and image segmentation. *Photogrammetric Engineering & Remote Sensing*, *70*(12), 1365-1371. https://doi.org/10.14358/pers.70.12.1365

Ural, S., Shan, J., Romero, M., & Tarko, A. (2015). Road and roadside feature extraction using imagery and LiDAR data for transportation operation. *ISPRS Annals of the Photogrammetry, Remote Sensing and Spatial Information Sciences*, *2*, 239-246. https://doi.org/10.5194/isprsannals-ii-3-w4-239-2015

Valero, S., Chanussot, J., Benediktsson, J. A., Talbot, H., & Waske, B. (2010). Advanced directional mathematical morphology for the detection of the road network in very high resolution remote sensing images. *Pattern Recognition Letters*, *31*(10), 1120-1127. https://doi.org/10.1016/j.patrec.2009.12.018

Yang, Y., Wu, Q., Yu, R., Wang, L., Zhao, Y., Ding, C., & Yin, Y. (2024). Intelligent road extraction from high resolution remote sensing images based on optimized SVM. *Journal of Radiation Research and Applied Sciences*, *17*(4), 101069. https://doi.org/10.1016/j.jrras.2024.101069

Yigit, A.Y., & Uysal, M. (2026). The effect of different areas and image band in the road extraction from high-resolution uav images

using the Obia method. *Applied Geomatics*, 18(33). https://doi.org/10.1007/s12518-025-00678-8

Zhang, Z., & Wang, Y. (2019). JointNet: A common neural network for road and building extraction. *Remote Sensing*, *11*(6), 696. https://doi.org/10.3390/rs11060696

This Page is Intentionally Left Blank